Analysis of Graphene Plasmonic Waveguides and Switching Components via a Finite Element Formulation with Surface Conductivity

I. Demirtzioglou and T. V. Yioultsis
Department of Electrical and Computer Engineering, Aristotle University of Thessaloniki
Thessaloniki 54124, Greece

Abstract— We present an efficient finite element formulation for the eigenmode analysis of graphene-based plasmonic waveguides with switching functionalities. The formulation is full-vectorial and addresses graphene as a surface conductivity, as opposed to bulky material considerations, thus eliminating the need for fine discretizations inside thin graphene models. Based on this technique technique, a graphene-enhanced plasmonic CGS waveguide with good extinction ratio and insertion loss is proposed.

1. INTRODUCTION

Graphene is a ground-breaking material, with a multitude of significant properties and effects, including the ability to support surface plasmon propagating modes and switching functionalities [1]. Optical conductivity of graphene has been shown to consist of a Drude intraband term and an interband contribution. These properties may result in either plasmonic modes in THz [2] or enhanced switching in photonic waveguides for the optical communications regime [3]. In particular, for the case of the THz regime, where the Drude term is dominant, graphene surface plasmons offer the possibility of waveguiding with strong confinement, while in the optical communications spectrum where the interband contribution is substantial, the tunability of graphene's conductivity through electrostatic gating shows great potential for the design of switching components.

Regarding FEM simulations of such structures, the general trend is often to approach graphene as a bulky material, thus requiring very fine descritizations inside thin graphene models but also in the surrounding space. We present here an efficient formulation for the eigenmode analysis of graphene-based plasmonic waveguides with switching functionalities which is full-vectorial and addresses graphene as a thin sheet with a surface conductivity. Based on this analysis, we propose a graphene-enhanced plasmonic CGS waveguide with an extinction ratio of 8.6 dB and a 2.15 dB insertion loss for a 10 μm length, which can be considered highly satisfactory and a firm basis for further study towards the development of switched plasmonic components in the photonics regime.

2. FINITE ELEMENT FORMULATION

The proposed finite element eigenmode formulation follows the general framework that has been proposed in [4], where the electric field is used as a working variable. The formulation uses mixed finite elements for the discretization of the waveguide cross section, with tangentially continuous (H-curl) vector finite elements in the transverse plane and scalar (nodal) finite elements for the axial component. Using the Galerkin formulation for the Helmholtz equation, the form

$$\iint\limits_S \mathbf{E}' \cdot \left(\nabla \times \overline{\overline{\mu_r^{-1}}} \nabla \times \mathbf{E} - k_0^2 \overline{\overline{\varepsilon_r}} \mathrm{E} \right) ds = 0 \tag{1}$$

expresses the projected problem, reducing its solution to a finite-dimensional vector subspace. The electric field can be written in the form $\mathbf{E} = (\mathbf{E}_t + \hat{\mathbf{z}} E_z)\, e^{-\gamma z}$, where $\mathbf{E}_t = \mathbf{E}_t(x, y)$ represents the transverse component and $E_z = E_z(x, y)$ represents the axial component. The adjoint field $\mathbf{E}' = (\mathbf{E}'_t - \hat{\mathbf{z}} E'_z)\, e^{\gamma z}$ is selected as the test function in the Galerkin equation and the final eigenmode formulation expressed as a function of the effective refractive index $n_{\mathit{eff}} = -j\gamma/k_0$ is as follows:

$$\iint\limits_S \nabla \times \mathbf{E}'_t \cdot \mu_{r,zz}^{-1} \nabla \times \mathbf{E}_t ds - \iint\limits_S \left(\nabla E'_z \times \hat{\mathbf{z}}\right) \cdot \overline{\overline{\mu_{r,tt}^{-1}}} \left(\nabla E_z \times \hat{\mathbf{z}}\right) ds - k_0^2 \iint\limits_S \mathbf{E}'_t \cdot \overline{\overline{\varepsilon_{r,tt}}} \mathbf{E}_t ds$$
$$+k_0^2 \iint\limits_S E'_z \cdot \varepsilon_{r,zz} E_z ds + n_{\mathit{eff}} \left[-jk_0 \iint\limits_S (\mathrm{E}'_t \times \hat{\mathbf{z}}) \cdot \overline{\overline{\mu_{r,tt}^{-1}}} (\nabla E_z \times \hat{\mathbf{z}}) ds - jk_0 \iint\limits_S \left(\nabla E'_z \times \hat{\mathbf{z}}\right) \cdot \overline{\overline{\mu_{r,tt}^{-1}}} \left(\mathrm{E}_t \times \hat{\mathbf{z}}\right) ds \right]$$
$$+n_{\mathit{eff}}^2 \left[k_0^2 \iint\limits_S \left(\mathrm{E}'_t \times \hat{\mathbf{z}}\right) \cdot \overline{\overline{\mu_{r,tt}^{-1}}} \left(\mathrm{E}_t \times \hat{\mathbf{z}}\right) ds \right] - \oint\limits_{\partial S} \mathbf{E}' \cdot \hat{\mathbf{n}} \times \nabla \times \mathbf{E} ds = 0 \tag{2}$$

The domain is terminated by perfectly matched layers. Following the discretization of the 2D-space, and assuming for the moment that the line integral vanishes, (2) can be easily written as the sum of the same surface integral quantities calculated for each element of the grid, leading to the expanded form of Galerkin formulation,

$$S_e^t - S_e^{z,m} - k_0^2 T_e^t + k_0^2 T_e^z + n_{\mathit{eff}} \left(-jk_0 P_e - jk_0 Q_e\right) + n_{\mathit{eff}}^2 \left(k_0^2 T_e^{t,m}\right) = 0 \tag{3}$$

where

$$S_e^t = \iint\limits_{S_n} \nabla \times \mathbf{E}'_t \cdot \mu_{r,zz}^{-1} \nabla \times \mathbf{E}_t ds, \quad S_e^{z,m} = \iint\limits_{S_n} \left(\nabla E'_z \times \hat{\mathbf{z}}\right) \cdot \overline{\overline{\mu_{r,tt}^{-1}}} \left(\nabla E_z \times \hat{\mathbf{z}}\right) ds,$$
$$T_e^t = \iint\limits_{S_n} \mathbf{E}'_t \cdot \overline{\overline{\varepsilon_{r,tt}}} \mathbf{E}_t ds, \quad T_e^z = \iint\limits_{S_n} E'_z \cdot \varepsilon_{r,zz} E_z ds, \quad T_e^{t,m} = \iint\limits_{S_n} \left(\mathrm{E}'_t \times \hat{\mathbf{z}}\right) \cdot \overline{\overline{\mu_{r,tt}^{-1}}} \left(\mathrm{E}_t \times \hat{\mathbf{z}}\right) ds, \tag{4}$$
$$P_e = \iint\limits_{S_n} \left(\mathrm{E}'_t \times \hat{\mathbf{z}}\right) \cdot \overline{\overline{\mu_{r,tt}^{-1}}} \left(\nabla E_z \times \hat{\mathbf{z}}\right) ds, \quad Q_e = \iint\limits_{S_n} \left(\nabla E'_z \times \hat{\mathbf{z}}\right) \cdot \overline{\overline{\mu_{r,tt}^{-1}}} \left(\mathrm{E}_t \times \hat{\mathbf{z}}\right) ds$$

The matrix formulation of the problem can be derived by substituting fields by their corresponding discrete expressions using basis functions and the degrees of freedom (nodal or edge-based, according to the field component) for the electric field quantities and ultimately takes the form

$$\left\{ \begin{bmatrix} \mathbf{S}^t - k_0^2 \mathbf{T}^t & 0 \\ 0 & -\mathbf{S}^{z,m} + k_0^2 \mathbf{T}^z \end{bmatrix} + n_{\mathit{eff}} \begin{bmatrix} 0 & -jk_0 \mathbf{P} \\ -jk_0 \mathbf{Q} & 0 \end{bmatrix} + n_{\mathit{eff}}^2 \begin{bmatrix} k_0^2 \mathbf{T}^{t,m} & 0 \\ 0 & 0 \end{bmatrix} \right\} \begin{bmatrix} \mathbf{E}_t \\ \mathbf{E}_z \end{bmatrix} = 0 \tag{5}$$

following an assembly process for the element quantities, where the matrices in (5) correspond to Galerkin terms in (4). Given that the eigenmode problem is mathematically interpreted as an eigenvalue calculation problem for the system of (5), the aim is to solve for n_{eff}. However, this eigenvalue problem is quadratic, so we use first companion linearization to reduce it to

$$\begin{bmatrix} 0 & 0 & \mathbf{I} & 0 \\ 0 & 0 & 0 & \mathbf{I} \\ -\mathbf{S}^t + k_0^2 \mathbf{T}^t & 0 & 0 & jk_0 \mathbf{P} \\ 0 & \mathbf{S}^{z,m} - k_0^2 \mathbf{T}^z & jk_0 \mathbf{Q} & 0 \end{bmatrix} \begin{bmatrix} \mathbf{E}_t \\ \mathbf{E}_z \\ n_{\mathit{eff}} \mathbf{E}_t \\ n_{\mathit{eff}} \mathbf{E}_z \end{bmatrix} = n_{\mathit{eff}} \begin{bmatrix} \mathbf{I} & 0 & 0 & 0 \\ 0 & \mathbf{I} & 0 & 0 \\ 0 & 0 & k_0^2 \mathbf{T}^{t,m} & 0 \\ 0 & 0 & 0 & 0 \end{bmatrix} \begin{bmatrix} \mathbf{E}_t \\ \mathbf{E}_z \\ n_{\mathit{eff}} \mathbf{E}_t \\ n_{\mathit{eff}} \mathbf{E}_z \end{bmatrix} \tag{6}$$

which is a sparse form with a positive semidefinite matrix at the right hand side, suitable for sparse eigensolvers.

As far as the graphene implementation is concerned, its extremely small thickness (one-atom thick) dictates its consideration as an ideal two-dimensional surface with a corresponding surface conductivity σ_g (measured in S). Therefore, any graphene surfaces in the waveguide eigenmode analysis are basically represented by one-dimensional lines in the 2D cross-section of the structures. A first route to incorporate graphene sheets in FEM simulations is to start from a bulky material approach and consider the limit of its thickness to zero. In thic case graphene's contribution would be apparent through its conductivity, thus affecting the 3rd and 4th term of (2) which include permittivity quantities. In these integrals, separating a finite surface of thickness δ corresponding to the bulky graphene area, we derive the additional terms

$$I_g = -k_0^2 \iint\limits_{S_1} \mathbf{E}'_t \cdot \overline{\overline{\varepsilon_{r,tt}}} \mathbf{E}_t ds + k_0^2 \iint\limits_{S_1} E'_z \cdot \varepsilon_{r,zz} E_z ds \tag{7}$$

where we replace the permittivity with the complex permittivity of graphene $\varepsilon_r^* = \varepsilon_r - j\sigma_b/\omega\varepsilon_0$, and σ_b describes an equivalent conductivity of bulk graphene (in S/m). Assuming that σ_b consists of non-zero real and imaginary parts, we can omit ε_r as being included in σ_b and have $\varepsilon_r^* = -j\sigma_b/\omega\varepsilon_0$. Therefore (7) becomes

$$I_g = jk_0\eta_0 \iint\limits_{S_1} \mathbf{E}'_t \cdot \sigma_b \mathbf{E}_t ds - jk_0\eta_0 \iint\limits_{S_1} E'_z \cdot \sigma_b E_z ds \tag{8}$$

Assuming an infinitesimal graphene thickness, variations are negligible in this dimension, giving

$$I_g = jk_0\eta_0 \int\limits_{\partial S} \mathbf{E}'_{t,p} \cdot \sigma_g \mathbf{E}_{t,p} dl - jk_0\eta_0 \int\limits_{\partial S} E'_z \cdot \sigma_g E_z dl \tag{9}$$

where $\delta\sigma_b$ equals the surface conductivity σ_g (in S). It has to be particularly noted that the electric field component $\mathbf{E}_{t,p}$ involved in the first integral is not the full transverse component but only its tangential projection on the one-dimensional graphene line.

An equivalent and more elegant way to arrive at the same expression is to consider graphene as a zero thickness sheet in the first place. In this case, the line integral term in (2) cannot be ignored, as the graphene current sheet introduces a discontinuity in the magnetic field, thus affecting the line integral term. In particular, the interface condition on the graphene sheet is written in the form

$$-\frac{j}{k_0\eta_0} \left(\hat{\mathbf{n}}_g \times \nabla \times \mathbf{E}^+ - \hat{\mathbf{n}}_g \times \nabla \times \mathbf{E}^- \right) = \mathbf{J}_s = \sigma_g \left(\mathbf{E}_{t,p} + \hat{\mathbf{z}} E_z \right) \tag{10}$$

where $\hat{\mathbf{n}}_g$ is the unit vector normal to the graphene sheet. However, to substitute (10) in the line integral term of (2) we need to consider a fictitious surface that surrounds the graphene sheet from both sides and being infinitely close to it. Therefore, the line integral is split into two parts, one for the upper surface, where the outward-pointing unit normal vector is $\hat{\mathbf{n}}^+ = \hat{\mathbf{n}}_g$ and one for the lower one, where $\hat{\mathbf{n}}^- = -\hat{\mathbf{n}}_g$ and the line integral takes the form

$$\begin{aligned} I_g &= \int\limits_{\partial S^+} \mathbf{E}' \cdot \hat{\mathbf{n}}^+ \times \nabla \times \mathbf{E}^+ ds + \int\limits_{\partial S^-} \mathbf{E}' \cdot \hat{\mathbf{n}}^- \times \nabla \times \mathbf{E}^- ds \\ &= \int\limits_{\partial S^-} \mathbf{E}' \cdot \hat{\mathbf{n}}_g \times \left(\nabla \times \mathbf{E}^+ - \nabla \times \mathbf{E}^- \right) ds = jk_0\eta_0 \int\limits_{\partial S^-} \mathbf{E}' \cdot \sigma_g \mathbf{E}_p ds \end{aligned} \tag{11}$$

which easily results in (9) as well.

Therefore, graphene's contribution can be implemented by adding two line integral terms in the initial formulation, expressed as

$$T_e^{t,g} = \int\limits_C \mathbf{E}'_{t,p} \cdot \sigma_g \mathbf{E}_{t,p} dl, \quad T_e^{z,g} = \int\limits_C E'_z \cdot \sigma_g E_z dl \tag{12}$$

and by considering the corresponding matrices, it results in the linear eigenvalue problem of the form

$$\begin{aligned} &\begin{bmatrix} 0 & 0 & \mathbf{I} & 0 \\ 0 & 0 & 0 & \mathbf{I} \\ -\mathbf{S}^t + k_0^2\mathbf{T}^t - jk_0\eta_0\mathbf{T}^{t,g} & 0 & 0 & jk_0\mathbf{P} \\ 0 & \mathbf{S}^{z,m} - k_0^2\mathbf{T}^z + jk_0\eta_0\mathbf{T}^{z,g} & jk_0\mathbf{Q} & 0 \end{bmatrix} \begin{bmatrix} \mathbf{E}_t \\ \mathbf{E}_z \\ n_{\mathit{eff}}\mathbf{E}_t \\ n_{\mathit{eff}}\mathbf{E}_z \end{bmatrix} \\ &= n_{\mathit{eff}} \begin{bmatrix} \mathbf{I} & 0 & 0 & 0 \\ 0 & \mathbf{I} & 0 & 0 \\ 0 & 0 & k_0^2\mathbf{T}^{t,m} & 0 \\ 0 & 0 & 0 & 0 \end{bmatrix} \begin{bmatrix} \mathbf{E}_t \\ \mathbf{E}_z \\ n_{\mathit{eff}}\mathbf{E}_t \\ n_{\mathit{eff}}\mathbf{E}_z \end{bmatrix} \end{aligned} \tag{13}$$

which is easily discretized by the same kind of mixed vector-nodal finite elements.

3. PLASMONIC AND SWITCHING COMPONENTS

The proposed formulation is able to analyze both plasmon graphene ribbon waveguides in the THz regime and a switching-capable waveguide structure for telecom applications, based on the CGS waveguide [5], which is properly enhanced by graphene.

3.1. Graphene Microribbon Waveguide

To fully test the functionality of our formulation, we analyzed a plasmon graphene microribbon waveguide in the THz regime proposed by Nikitin et al. [2]. This is a waveguiding structure for frequencies between 1 and 12 THz (as opposed to the telecommunications wavelength regime) taking advantage of the surface conductivity of a graphene microribbon. The analysis was conducted for ribbon widths of 5 μm and 20 μm and the electric field intensity plots for the two transverse components, vertical (upper plots) and horizontal (lower plots) are shown, for the three first modes of the 5 μm ribbon, in Fig. 1.

The dispersion diagrams for the real part of the effective refractive index along with the propagation length are shown in Fig. 2 for the 5 μm case and are consistent with those in [2].

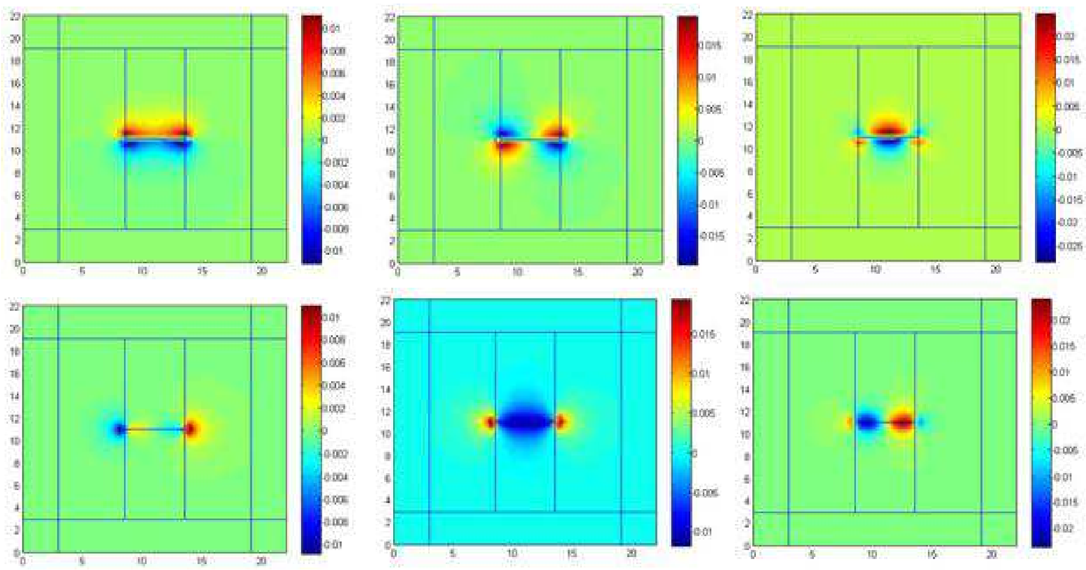

Figure 1: Mode profiles for the first three modes of a 5 μm graphere ribbon waveguide: vertical E-field component (upper plots) and horizontal E-field component (lower plots).

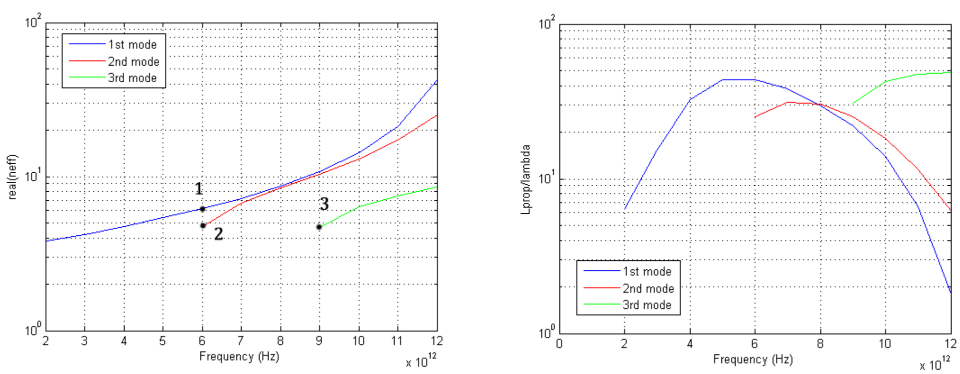

Figure 2: Dispersion diagrams: real part of the effective refractive index and propagation length for the 5 μm case.

3.2. Graphene Waveguide with High-index Dielectric Ridge

The next structure simulated was the graphene waveguide proposed in [3]. Its concept takes advantage of a high-index dielectric ridge to achieve strong field confinement without using a finite

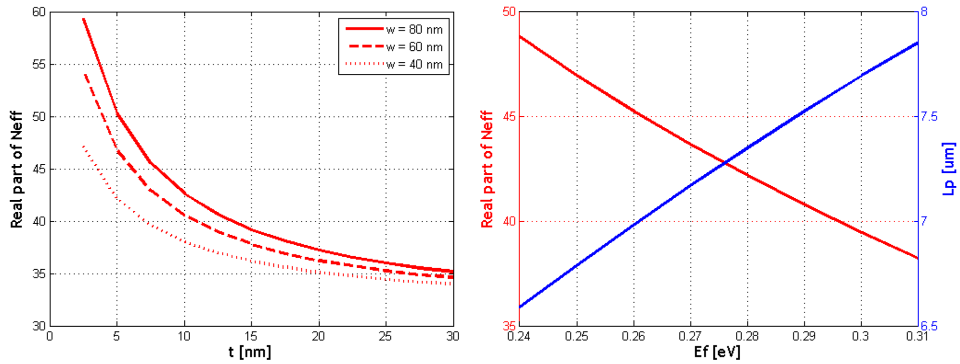

Figure 3: Real part of the effective refractive index with respect to gap thickness and chemical potetntial.

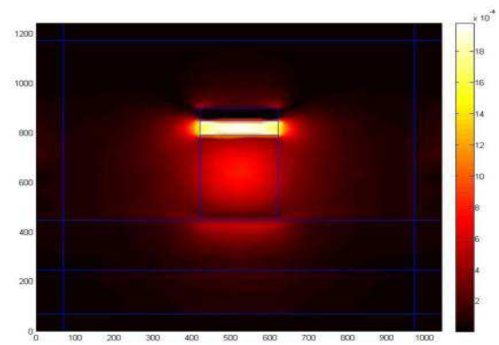

Figure 4: Graphene-enhanced CGS waveguide (dominant mode).

width graphene ribbon which is harder to fabricate. Placing a wide graphene sheet over a dielectric ridge of appropriate size, the geometry of the structure facilitates waveguiding. The relation of the complex effective refractive index to the thickness of gap the graphene sheet and the dielectric ridge, as well as to the chemical potential are shown in Fig. 3, being in very good agreement with [3].

3.3. Graphene Switching Component

Based on the analysis, we propose a switching capability for the classic plasmonic CGS waveguide [5, 6] by adding graphene layers on all interfaces between waveguide materials, including both sides of the oxide layer, and also the two vertical ridges of the waveguide (Fig. 4). The ON and OFF states of the waveguide correspond to chemical potential values 1 eV and 0.1 eV. Selecting a structure length of 10 μm, the insertion loss can be as low as 2.15 dB, almost entirely due to metal (not graphene) losses and the achieved extinction ratio is 8.6 dB, which is highly promising for further study.

REFERENCES

1. Bludov, Y. V., A. Ferreira, N. M. R. Peres, and M. I. Vasilevskiy, "A primer on surface plasmon-polaritons in graphene," *Int. J. Mod. Phys. B*, Vol. 27, 1341001, 2013.
2. Nikitin, A. Y., F. Guinea, and F. J. García-Vidal, "Edge and waveguide terahertz surface plasmon modes in graphene microribbon," *Phys. Rev. B*, Vol. 84, 161407(R), 2011.
3. Sun, Y., Z. Zheng, J. Cheng, and J. Liu, "Graphene surface plasmon waveguides incorporating high-index dielectric ridges for single mode transmission," *Optics Communications*, Vol. 328, 124–128, 2014.
4. Selleri, S., L. Vincetti, A. Cucinotta, and M. Zoboli, "Complex FEM modal solver of optical waveguides with PML boundary conditions," *Optical and Quantum Eletronics*, Vol. 33, No. 4–5, 359–371, 2001.
5. Dai, D. and S. He, "A silicon-based hybrid plasmonic waveguide with a metal cap for a nano-scale light confinement," *Optics Express*, Vol. 17, No. 19, 2009.
6. Wu, M., Z. Han, and V. Van, "Conductor-gap-silicon plasmonic waveguides and passive components at subwavelength scale," *Optics Express*, Vol. 18, No. 11, 11728–11736, 2010.